Catastrophic and noncatastrophic population crashes in a bitrophic system with dynamic additional food provision to cooperative predators

Saswati Biswas,[1] Arindam Mandal,[2] and Samares Pal[3,*]
[1]Department of Mathematics, School of Natural Sciences, Shiv Nadar Institution of Eminence,
Gautam Buddha Nagar, Uttar Pradesh 201314, India
[2]Department of Mathematics, Indian Institute of Technology Ropar, Rupnagar 140001, Punjab, India
[3]Department of Mathematics, University of Kalyani, Kalyani 741235, India

(Received 18 July 2023; accepted 1 February 2024; published 28 February 2024)

In this article we contemplate the dynamics of an additional food-provided prey-predator system. We assume that the behavior of cooperative predators induces fear in prey, which radically affects the prey's birth and death rates. We observe that the structural instability imposed by strong cooperative hunting among predators goes away with higher intensities of fear levels affecting the prey's reproductive output and mortality. High levels of prey refuge are not conducive to the survival of predators. In such a situation, adequate supply of high-quality additional food is favorable regarding the persistence and stability of the system. Interestingly, the system potentially exhibits two stable configurations under identical ecological conditions by allowing different bifurcation scenarios, including saddle-node and backward bifurcations, and associated hysteresis effects with prey refuge along with additional food quantity and quality. In the stochastic environment, the system experiences critical transitions through bifurcation-induced tipping events with time-varying additional food for predators. Enhanced disturbance events promote noise-induced switching and tipping events. Finally, our investigation explores whether impending population crashes resulting from the variability of additional food quantity and quality can reliably be predicted using early warning signals in the context of redshifted noise. Overall, our results may provide insights for finding control strategies in the context of community ecology.

DOI: 10.1103/PhysRevE.109.024224

I. INTRODUCTION

Predator-prey interplay has been a predominant and active research area for both mathematicians and ecologists for the past few decades. Mathematical models provide researchers with a means to consolidate knowledge, test hypotheses, and employ nonlinear differential equations for qualitative and quantitative modeling of terrestrial ecosystems [1]. Additionally, numerical simulations utilizing differential equations can effectively encompass the impact of physical, chemical, and biological processes associated with population dynamics, either individually or in combination. This approach helps simplify the complexity of diverse ecological configurations [2].

To achieve collective success in hunting, predators are expected to embrace cooperative behavior. Such ubiquitous social interactions help the predator population raise their effective consumption to the optimal level. The likelihood of successful shared hunting increases with an expanding adult pack [3]. However, there may be differences among individuals in the degree to which communal hunting is beneficial or harmful. In ecology, species interactions are not always governed through direct predation; sometimes the nonconsumptive fear effect due to perceived threat of predation can be more influential in shaping the overall ecosystem functioning by altering the behavioral and physiological aspects of prey species. To cope with predation risk, prey evolves to adopt different survival strategies such as alterations in foraging behavior, patterns of aggregation, habitat selection, reproductive tactics, vigilance periods, etc., all of which undeniably impact their physiological condition. These effects can manifest as increased blood sugar levels, heightened emotional arousal, activation of stress hormone secretion, and other related physiological responses. In the high-risk zone, restricted foraging activities compel the scared prey to feed on a low-quantity diet. For example, fearful mule deer adopt minimal foraging to circumvent the risk of predation of the mountain lion [4]. The inevitable stress of prolonged starvation leads to reduced prey reproduction and lessens the adult survivability. To avoid the predation risk, prey often find their way out by moving from their optimal territory to new habitats with lower quality, incurring an energy loss in the process [5]. Hua *et al.* [6] found that perception of predation risk negatively impact the blue bird's reproductive physiology by broadcasting the vocal cues of their consumers.

The pioneering work by Wang *et al.* [7], demonstrating the fear phenomenon in mathematical perspective, established that strong fear possesses a stabilizing role by ruling out periodic oscillations, whereas relatively weak fear may produce multistability in a bitrophic model. Recently, empirical investigations have been undertaken to explore the infection dynamics in ecological systems incorporating the impact of fear [8,9]. Duarte *et al.* [10] studied a three-tier

---

[*] samaresp@yahoo.co.in

food chain with hunting cooperation among predators. Alves and Hilker [11] discussed a Lotka-Volterra model with cooperative predators and demonstrated how cooperation can alter prey-predator dynamics. Recently, Pal *et al.* [12] studied the simultaneous impacts of cooperative hunting and the fear phenomenon in a classical prey-predator system and concluded that foraging facilitation in the form of hunting cooperation has the potential to induce a strong demographic Allee effect in predators. Liu *et al.* [13] proposed and analyzed a fear-induced eco-epidemiological model with cooperative predators. Their findings suggested that low levels of hunting cooperation and fear factor can stabilize the disease-dominated system, whereas relatively high levels of these model parameters can induce a periodic phenomenon.

In response to the evading risk of predation, prey species actively embrace a defense against the predators by taking refuge. This hiding behavior provides them with some degree of protection from potential predators and reasonably promotes the chance of prey survivability. Prey refuge has various potential impacts on the dynamics of prey-predator interactions, including promoting stability, generating dynamic fluctuations, or inducing instability in an ecosystem functioning [14]. For example, zooplankton frequently try to escape from pelagic consumers using macrophytes as daytime refuge sites [15]. The foraging behaviors of zooplankton vary based on the states and compositions of the resources that are accessible to them [16–18]. It is observed that prey refuge is capable of diluting the oscillatory tendency of predator-prey interactions and fosters the stabilization of community equilibria. Sharma *et al.* [19] studied the effects of prey refuge in a prey-predator Leslie-Gower model with prey infection and showed that prey refuge is responsible for the emergence and termination of population outbreaks. McNair [20] documented that a variety of refuges could impose a locally destabilizing role and generate stable large-amplitude periodic solutions, which would wipe out the population in the absence of refuge. Kar [21] suggested that a high level of refuge can increase prey population densities, which serve as a key factor for the emergence of population outbreaks.

The inclusion of supplementary food has emerged as a highly effective approach in the realm of biological conservation and pest management [22–24]. Adequate provision of additional food plays a crucial role in enhancing the lifespan, reproductive capacity, and overall ability of predator populations to regulate the proliferation of pests [25,26]. Predators possess an inherent propensity towards alternative diets when the primary prey becomes scarce in numbers. This preference for alternative food sources aids in the prolonged survival of predators. A notable example occurred in the mid 1990s when the populations of three subspecies of Channel Island foxes were on the verge of extinction due to excessive predation by golden eagles. In this scenario, the presence of plentiful alternative resources played a crucial role in the revitalization of fox populations [27]. Srinivasu *et al.* [28] reported the crucial impacts of both quantity and quality of available additional food items on the dynamics of the predator-prey system. Mandal *et al.* [29] documented the effects of phytoplankton refuge on the dynamical complexities of an additional food-provided phytoplankton-zooplankton system with seasonality. Sahoo and Poria [30] revealed that a suitable quantity of higher-quality additional food for the top predator can eliminate the chaotic disorder in a tritrophic ecological food chain model. Mandal *et al.* [31] investigated an additional food-provided phytoplankton-zooplankton system in the presence of anthropogenic toxicants.

The functionality of additional food within predator-prey ecosystems can be analogized to various mechanisms at play in climate, healthcare, and social systems. To illustrate, we consider geoengineering, which entails deliberate interventions in the earth's climate system to mitigate the effects of climate change. The process of injecting aerosols into the stratosphere to reflect sunlight and lower the temperature, thereby offsetting the impact of greenhouse gases [32], bears resemblance to the introduction of additional food in predator-prey ecosystems. In the realm of healthcare systems, vaccination campaigns can be likened to the introduction of additional immunity into a population to curtail the disease burden [33]. In this scenario, vaccinations bolster the "immunity" of the host population against the "predator" pathogen. A comparable analogy can be drawn in the aftermath of natural disasters or crises. The provision of aid, resources, and support can function as a buffer [34], akin to the introduction of additional food in predator-prey systems, facilitating communities' recovery and the restoration of steady states. Recognizing these parallels allows us to draw lessons on societal resilience in the face of disruptions, broadening the discourse beyond ecological contexts.

Here we provide an illustration of a real-world situation that unfolds different layers of predator-prey interactions. In the Elysian Forest, interplay between two groups of animals, the shadow-stalker predators (panthers, wolves, owls, etc.) and the watchful prey (deer, rabbits, squirrels, etc.), is commonly evidenced. The shadow stalkers have mastered their hunting skills and developed a remarkable form of cooperation using body language and soft vocalizations. This coordination instills fear in the prey, who seek refuge in temporary shelters until they perceive the danger has passed. When prey is scarce, the shadow stalkers adapt by scavenging and hunting smaller creatures, ensuring they have a food source even when their focal prey is in hiding. In this ecosystem, predator and prey coexist, adapting to nature's rhythms and maintaining a delicate balance in the forest.

Motivated by this, we explore the notion that predators engage in cooperative hunting to enhance their hunting accuracy. This substantially impacts the behavior and physical characteristics of prey species as the fear of predation pressure comes into play. The prey species use refuge as a defensive strategy to suppress the exogenous impact of fear of predation. In such a situation, limited availability of the focal prey influences the predator population's switching behavior to other resources as a survival hack.

Random environmental fluctuations play a pivotal role in understanding ecological systems and can have significant implications for the persistence and and stability of the community. The interplay between nonlinearity and stochasticity in a system adds complexity, particularly in cases of bistability, making it an intriguing area of investigation [35,36]. This motivates us to investigate the stochastic counterpart of the proposed ecological model. Additionally, we explore the potential of generic early warning signals to predict impending state transitions in an environment with variations in both quantity and quality of additional food resources.

II. MATHEMATICAL MODEL

At any time $t > 0$, let $N(t)$ and $P(t)$ be the densities of basal prey and predator populations, respectively. Now we present the ecological model, taking into account specific assumptions.

(i) In the absence of a predator, the focal prey follows a logistic growth pattern.

(ii) To account for the interaction between the focal prey and predator, we introduce a generalized type II interaction that incorporates an additional food supplement. We also assume that the predator's encounter rate with a basal resource increases with predator density, capturing the idea of cooperative hunting. This is achieved by modeling the effectual encounter rate as $q(P) = q + \alpha P$, where α quantifies the degree of cooperation among predators [11].

(iii) Predator cooperative hunting leads to a neuropsychological stress response in fearful prey, which is ecologically manifested as a reduction in their birth rate. We express the effective birth rate employing a decreasing function $a(k_1, \alpha, P) = \frac{a}{1+k_1\alpha P}$ [7]. However, the prey's death rate increases in the presence of chronic stress induced by the fear of predation. Mathematically, we capture this phenomenon by multiplying the death rate c of prey with an increasing function of predator population size $\phi(k_2, \alpha, P) = 1 + k_2\alpha P$ [37]. The parameters k_1 and k_2 signify the costs of fear of predation.

(iv) A constant proportion $m \in [0, 1)$ of prey individuals temporarily hide themselves in a less accessible zone to lower the chance of being attacked. This leaves $(1 - m)N$ unprotected basal resources available for predator consumption.

(v) The additional food is assumed to be nondynamic in nature. The number of encounters per predator with available additional food is directly proportional to the food biomass [28]. If $h_A(h_N)$ and $e_A(e_N)$ encapsulate the handling time of the predator per unit quantity of additional food (basal prey) and searching efficiency of the predator for the additional food (basal prey), respectively, then $q = 1/h_N$, $1/\delta = 1/e_N h_N$, $\beta_1 = h_A/h_N$, and $\mu = e_A/e_N$. The parameter β_1 measures the quality of the additional food available for the predator population while μ represents the efficacious capability of the predator to detect the additional food resources relative to the focal prey. If the inequality $h_A < h_N$ holds, we can infer that the additional food item is of higher quality. Therefore, for higher-quality additional food, β_1 should be less than unity. The uniform distribution of constant additional food biomass is sustained either by some external resources or by nature itself.

Based on the aforementioned assumptions, we propose the following nonlinear ecological system (see also Table I):

$$\begin{aligned}\frac{dN}{dt} &= \frac{aN}{1+k_1\alpha P} - c(1+k_2\alpha P)N - d_1N^2\\&\quad - \frac{(1-m)(q+\alpha P)NP}{1+\delta(1-m)(q+\alpha P)N+\beta_1\mu A},\\\frac{dP}{dt} &= \frac{\lambda[(1-m)(q+\alpha P)N+\mu A]P}{1+\delta(1-m)(q+\alpha P)N+\beta_1\mu A} - eP - d_2P^2.\end{aligned} \tag{1}$$

III. MATHEMATICAL ANALYSIS

Now we analyze several fundamental dynamical characteristics of the system (1), including positivity and boundedness of solutions, as well as local stability of the system's equilibria.

A. Positivity and boundedness of solutions

Lemma. The system (1) is positively invariant and bounded in $\mathbb{R}_+^2$ and the solutions eventually enter the attracting set

$$\Omega = \{(N, P) \in \mathbb{R}_+^2 : 0 \leqslant N + P \leqslant L\},$$

which is positively invariant.

Proof. From the system (1) we have

$$N(t) = N(0)\exp\int_0^t\left(\frac{a}{1+k_1\alpha P(x)} - c[1+k_2\alpha P(x)] - d_1N(x) - \frac{(1-m)[q+\alpha P(x)]P(x)}{1+\delta(1-m)[q+\alpha P(x)]N(x)+\beta_1\mu A}\right)dx,$$

$$P(t) = P(0)\exp\int_0^t\left(\frac{\lambda\{(1-m)[q+\alpha P(x)]N(x)+\mu A\}}{1+\delta(1-m)[q+\alpha P(x)]N(x)+\beta_1\mu A} - e - d_2P(x)\right)dx.$$

Therefore, the solutions of the model (1) are positive for all $t > 0$.

Define a function $U = N + P$. For an arbitrary $\sigma > 0$ we obtain

$$\frac{dU}{dt} + \sigma U \leqslant (a - c + \sigma)N - d_1N^2 - (e - \lambda\mu A - \sigma)P.$$

Choosing $\sigma \leqslant e - \lambda\mu A$, we have, for some M,

$$\frac{dU}{dt} + \sigma U \leqslant \frac{(a-c+\sigma)^2}{4d_1} = M.$$

Using the standard results of differential inequalities, we have, for some L,

$$U(t) \leqslant e^{-\sigma t}\left(U(0) - \frac{M}{\sigma}\right) + \frac{M}{\sigma} \leqslant \max\left\{\frac{M}{\sigma}, U(0)\right\} = L.$$

Hence, the solutions of the system (1) are ultimately bounded above.

This analytical method ensures that the interacting populations cannot grow indefinitely. ■

TABLE I. Biological meaning of the model parameters and their values.

Parameter	Description	Value
a	Birth rate of prey	0.28
c	Natural death rate of prey	0.12
k_1	Strength of fear due to cooperative hunting responsible for reduced prey reproduction	0.05
k_2	Strength of fear due to cooperative hunting responsible for elevated death rate among prey	0.05
d_1	Rate of intraspecies competition of prey	0.1
d_2	Mortality rate of predators due to crowding	0.05
e	Natural death rate of predator	0.1
m	Proportion of prey refuge	0.12
q	Attack rate of the predator on prey	0.25
α	Strength of cooperative hunting	0.65
β_1	Ratio between the handling times towards the additional food resources and the basal prey	0.15
μ	Effectual ability of predator to detect the additional food item relative to the basal prey	0.21
A	Quantity of available additional food	0.15
λ	Effectual rate of conversion of food to predator biomass	0.56
δ	Half-saturation constant	0.45

B. System's equilibria

Now we examine the feasible equilibria of the system and investigate the impact of key parameters on their local stability properties.

The system (1) possesses the following four ecologically meaningful equilibria.

(i) The population-free equilibrium $E_0 = (0, 0)$, which exists unconditionally. This is an undesired ecological scenario.

(ii) The predator-free equilibrium $E_1 = (N_1, 0)$, where $N_1 = \frac{1}{d_1}(a - c)$. The equilibrium E_1 exists, provided $a > c$. Ecologically, the prey species survives in the absence of potential predators only if the birth rate of the prey is greater than its mortality rate. In such a situation, the prey attains its carrying capacity N_1.

(iii) The prey-free equilibrium $E_2 = (0, P_2)$, where $P_2 = \frac{1}{d_2}(\frac{\lambda\mu A}{1+\beta_1\mu A} - e)$. The equilibrium E_2 exists if $A > A_c = \frac{e}{\mu(\lambda - e\beta_1)}$. Biologically, the predator population can manage to survive in the absence of focal prey if the accessible stock of additional food is greater than some level, which depends on the additional food quality β_1. Interestingly, as the food quality decreases, the minimum required quantity of additional food for predator survivability increases.

(iv) The coexisting equilibrium $E^* = (N^*, P^*)$, where N^* and P^* are the positive solutions of the nullclines:

$$f_1(N,P) \equiv \frac{a}{1+k_1\alpha P} - c(1+k_2\alpha P) - d_1 N - \frac{(1-m)(q+\alpha P)P}{1+\delta(1-m)(q+\alpha P)N+\beta_1\mu A} = 0, \quad (2)$$

$$f_2(N,P) \equiv \frac{\lambda[(1-m)(q+\alpha P)N+\mu A]}{1+\delta(1-m)(q+\alpha P)N+\beta_1\mu A} - e - d_2 P = 0. \quad (3)$$

Therefore, the equilibrium densities at the coexisting steady state correspond to the intersection between the nontrivial prey nullcline $f_1(N, P) = 0$ and the predator nullcline $f_2(N, P) = 0$ in the first quadrant.

Local stability analysis

Due to nonlinearity of the ecological system, it is quite impossible to find the exact solution to the system. Instead, we study the long-term dynamical behaviors of the system. Generally, a nonlinear system either gravitates towards an equilibrium point (steady state) or blows up. Here we adopt the linearization technique to study the local behaviors of the solution trajectories.

The Jacobian of the system (1) is given by $J = \begin{pmatrix} J_{11} & J_{12} \\ J_{21} & J_{22} \end{pmatrix}$, where

$$\begin{aligned}
J_{11} &= \frac{a}{1+k_1\alpha P} - c(1+k_2\alpha P) - 2d_1N \\
&\quad - (1-m)(1+\beta_1\mu A)(q+\alpha P)P\Lambda^2, \\
J_{12} &= -\frac{ak_1\alpha N}{(1+k_1\alpha P)^2} - ck_2\alpha N - (1-m)N\{[1+\delta(1-m) \\
&\quad \times (q+\alpha P)N + \beta_1\mu A](q+\alpha P) + (1+\beta_1\mu A)\alpha P\}\Lambda^2, \\
J_{21} &= \lambda(1-m)(q+\alpha P)[1+(\beta_1-\delta)\mu A]P\Lambda^2, \\
J_{22} &= \lambda\Bigg([(1-m)(q+\alpha P)N+\mu A]\frac{1}{\Lambda} \\
&\quad + \alpha(1-m)[1+(\beta_1-\delta)\mu A]NP\Bigg)\Lambda^2 - e - 2d_2P,
\end{aligned}$$

with $\Lambda = [1+\delta(1-m)(q+\alpha P)N+\beta_1\mu A]^{-1}$.

The Jacobian J_{E_0} at equilibrium E_0 has eigenvalues $(a - c)$ and $\frac{\lambda\mu A}{1+\beta_1\mu A} - e$. Therefore, for stability, we must have $a < c$ and $A < A_c$. Biologically, if the birth rate of the basal prey is less than their mortality rate, the prey fail to survive. In such a situation, inadequate supply of additional food drives the predator to go extinct.

The Jacobian J_{E_1} possesses eigenvalues $\frac{\lambda((1-m)qN_1+\mu A)}{1+\delta(1-m)qN+\beta_1\mu A} - e$ and $-(a - c)$. Thus, for stability $A < \frac{d_1e-q(a-c)(1-m)(\lambda-e\delta)}{d_1\mu(\lambda-e\beta_1)}$. From a biological viewpoint, an ecosystem can reach a state devoid of predators when the quantity of additional food supplied falls below a certain threshold. This threshold value is contingent upon the size of the prey refuge m. When a larger number of prey seek refuge, the minimum necessary food quantity increases accordingly, which is evident from the condition of local asymptotic stability of the predator-free equilibrium E_1.

The Jacobian J_{E_2} has the eigenvalues $\frac{\lambda\mu A}{1+\beta_1\mu A} - 2d_2P_2 - e$ and $\frac{a}{1+k_1\alpha P_2} - c(1 + k_2\alpha P_2) - \frac{(1-m)(q+\alpha P_2)P_2}{1+\beta_1\mu A}$. Therefore, the equilibrium E_2 is locally asymptotically stable, provided

$$m < 1 - \frac{1+\beta_1\mu A}{(q+\alpha P_2)P_2}\left(\frac{a}{1+k_1\alpha P_2} - c(1+k_2\alpha P_2)\right).$$

Biologically, cooperative predators can maximize their utilization of the primary resource if the prey population is unable to seek extensive refuge. Additionally, the refuge threshold is influenced by the quantity of supplementary food available. When predators receive a greater supply of

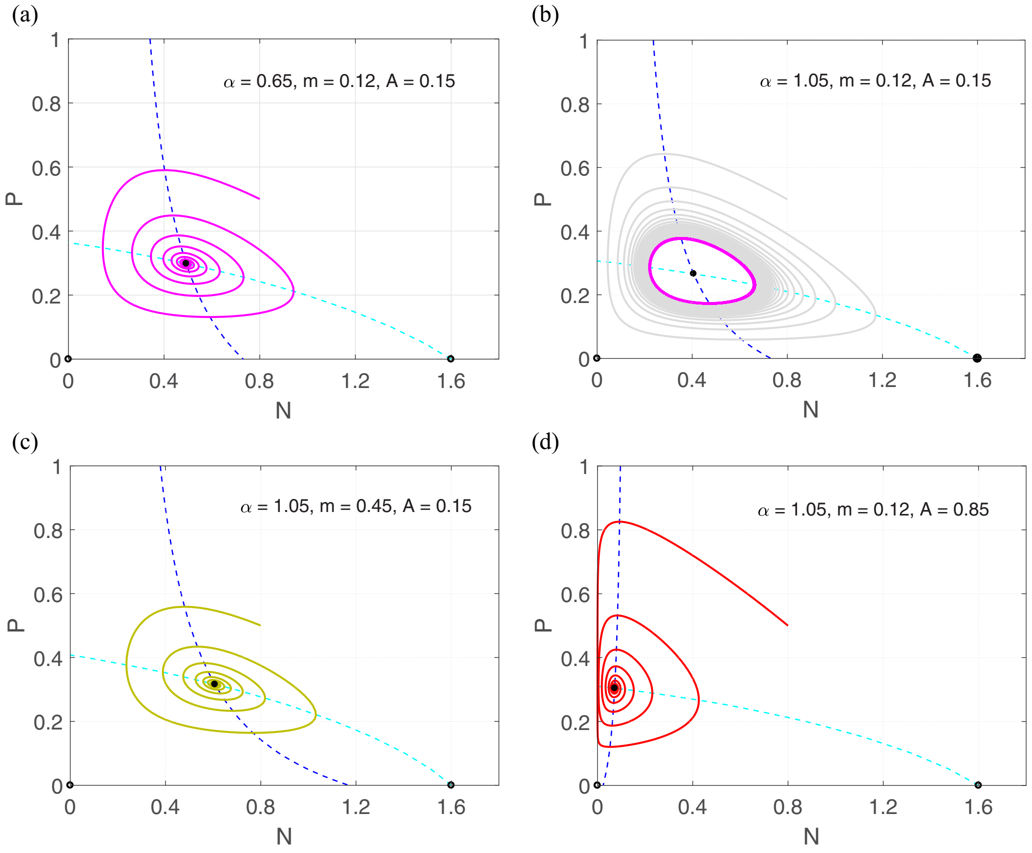

FIG. 1. Phase portraits of the system (1). The parameters are at default levels except for (b) $\alpha = 1.05$, (c) $\alpha = 1.05$ and $m = 0.45$, and (d) $\alpha = 1.05$ and $A = 0.85$. Cyan and blue dashed curves represent the prey and predator nullclines, respectively.

extra sustenance, their numbers increase, intensifying predation pressure and ultimately leading to the potential extinction of prey species. An alternative approach to rectify this detrimental scenario is for prey to seek greater refuge.

The Jacobian J_{E^*} is given by

$$J_{E^*} = \begin{pmatrix} c_{11} & c_{12} \\ c_{21} & c_{22} \end{pmatrix},$$

where $c_{ij} = J_{ij}$ at E^* except $c_{11} = \frac{\delta(1-m)^2(q+\alpha P)^2 PN}{\{1+\delta(1-m)(q+\alpha P)N+\beta_1\mu A\}^2} - d_1 N$. The characteristic equation is given by

$$\xi^2 + C_1\xi + C_2 = 0, \tag{4}$$

where $C_1 = -(c_{11} + c_{22} + c_{33})$ and $C_2 = c_{11}c_{22} - c_{12}c_{21}$. By the Routh-Hurwitz criterion, the roots of Eq. (4) have negative real components if and only if $C_1 > 0$ and $C_2 > 0$.

IV. SIMULATION RESULTS

In this section we provide some numerical results to further reveal the impacts of several key parameters on the resulting dynamics of the system (1).

Mathematical complexity restricts us to derive the expressions for the coexistence equilibria explicitly in terms of the key parameters. Figure 1 illustrates that the nullclines intersect precisely once, indicating the appearance of a unique coexisting equilibrium $E^* = (N^*, P^*)$ for appropriate parameter configurations. The system possesses stable dynamics at the unique interior equilibrium level $E^*(0.4926, 0.2985)$ [Fig. 1(a)]. An increase in the strength of hunting cooperation produces periodic phenomenon around the equilibrium $E^*(0.4055, 0.2663)$ [Fig. 1(b)]. The refuge by prey m and the quantity of additional food A potentially suppress the instability of the system, when increased to certain levels [Figs. 1(c) and 1(d)].

Figure 2 represents the changes in equilibrium densities of predator and prey populations by varying additional food quantity and quality, which prognosticate that higher amounts of additional food decrease the basal prey population. For a higher quantity of additional food, as the quality of the food continues to decrease, predator biomass increases to a certain level and then experiences a significant decline.

A. Stability behavior of the system

Figure 3(a) shows that two nontrivial nullclines $f_1(N, P)$ and $f_2(N, P)$ intersect at exactly two points in the interior of the first quadrant. The phase portrait diagram depicts the bistability phenomenon, where the system possesses two attractors, namely, $E_1 = (1.6, 0)$ and $E_1^* = (0.95, 0.3)$. We observe that, for the same parametric setup, green trajectories converge to the predator-free equilibrium E_1, whereas gray trajectories settle to the coexisting equilibrium E_1^*. However, Fig. 3(b) supports the monostability of the system at the coexisting steady state $E^*(0.19, 0.53)$ as the nearby trajectories approach the attractor.

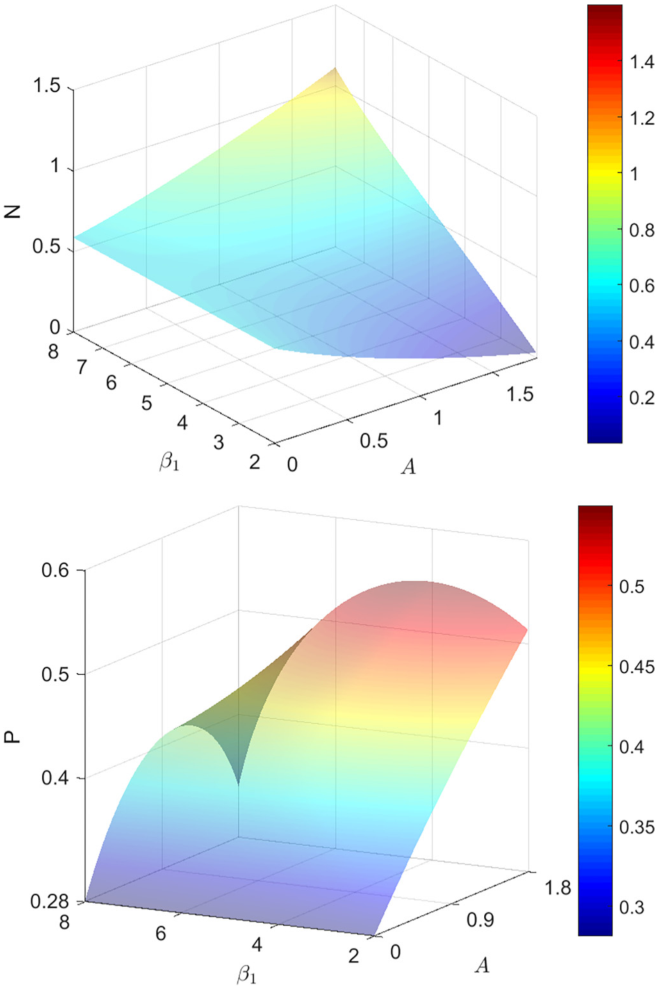

FIG. 2. Dependence of prey N^* and predator P^* equilibrium biomasses on quantity A and quality β_1 of additional food.

1. Increase in additional food quantity reduces probability of predator extinction

Now we consider a scenario in which the energy flow from focal prey cannot maintain survivability of potential predators in the absence of additional food. To observe the occurrence of backward bifurcation of the system (1) between the predator-free equilibrium and the coexisting equilibrium with respect to the quantity of additional food, we vary the parameter A in the interval [0,1.2] and plot the equilibrium densities of the predator population [Fig. 4(a)]. In this representation, we depict the stable branches of the boundary (predator-free and additional food dominated) and coexisting equilibria as blue straight lines and the blue curve, respectively; their unstable counterparts are represented by red straight lines and the red curve, respectively. The bifurcation diagram depicts that predator population does not survive for $A < 0.1157$ (region I). However, predators benefit from increasing additional food quantity. As a consequence, their equilibrium density is enhanced. We observe that there exists an interval $0.1157 < A < 0.2978$ for which a stable interior equilibrium coexists with the stable predator-free equilibrium (region II). Therefore, in this region the system displays susceptibility to small perturbations. At $A = A^* = 0.2978$, the unstable branch of the coexisting equilibrium meets the predator-free attractor and the equilibrium E_1 loses stability, yielding a backward bifurcation. For $A \in (0.2978, 1.1305)$, the system exhibits a unique coexisting attractor (regions III and IV). As A surpasses the threshold $\hat{A} = 1.1305$, the predator density reaches a plateau and a stable prey-free steady state originates from the former via a transcritical bifurcation. For $A > 1.1305$, the system exhibits monostability at the prey-free steady state E_2 (region V). Biologically, a large abundance of additional food may result in a significant increase in predator density that substantially leads to overexploitation of prey. In this situation, prey experience complete eradication from the ecosystem. To enhance the understanding of the bistability phenomenon, we draw the basins of attraction of the predator-free and coexisting equilibria for different levels of additional food [Figs. 4(b) and 4(c)]. Notably, the time evolutions starting from the blue region eventually converge to the predator-free equilibrium E_1, while for initial densities in the green region, the time evolutions settle to the coexisting equilibrium E_1^*. It is worth noting that the quantity of additional food significantly increases the domain of the basin

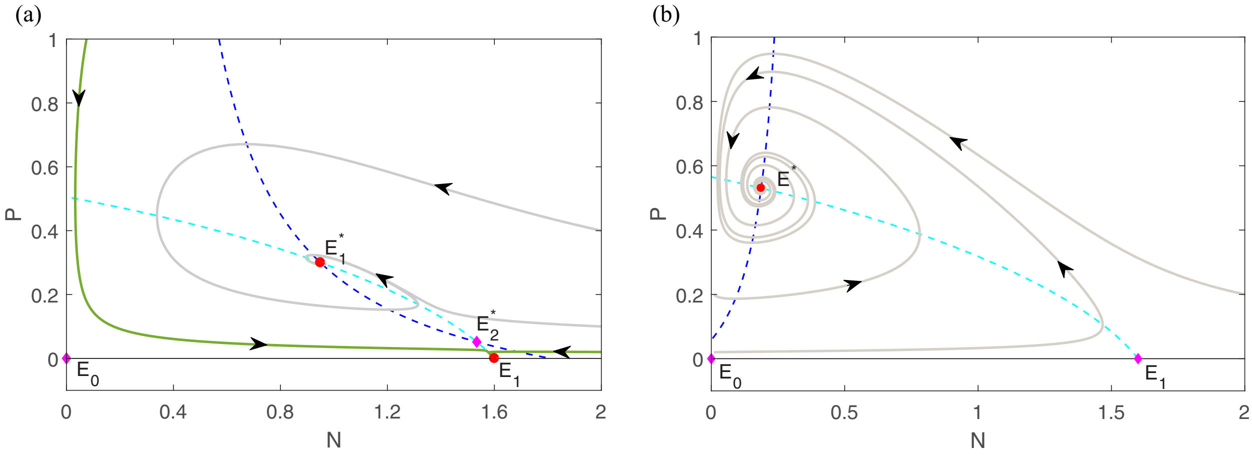

FIG. 3. (a) Bistability of the equilibria $E_1(1.6, 0)$ and $E_1^*(0.95, 0.3)$. (b) Monostability of the equilibrium $E^*(0.19, 0.53)$. The parameters are at the same levels as in Table I except for (a) $m = 0.62$, $\alpha = 1.05$, and $A = 0.1$ and (b) $m = 0.68$, $\alpha = 1.05$, and $A = 0.9$. Here red circles and magenta diamonds correspond to the stable and unstable equilibria, respectively.

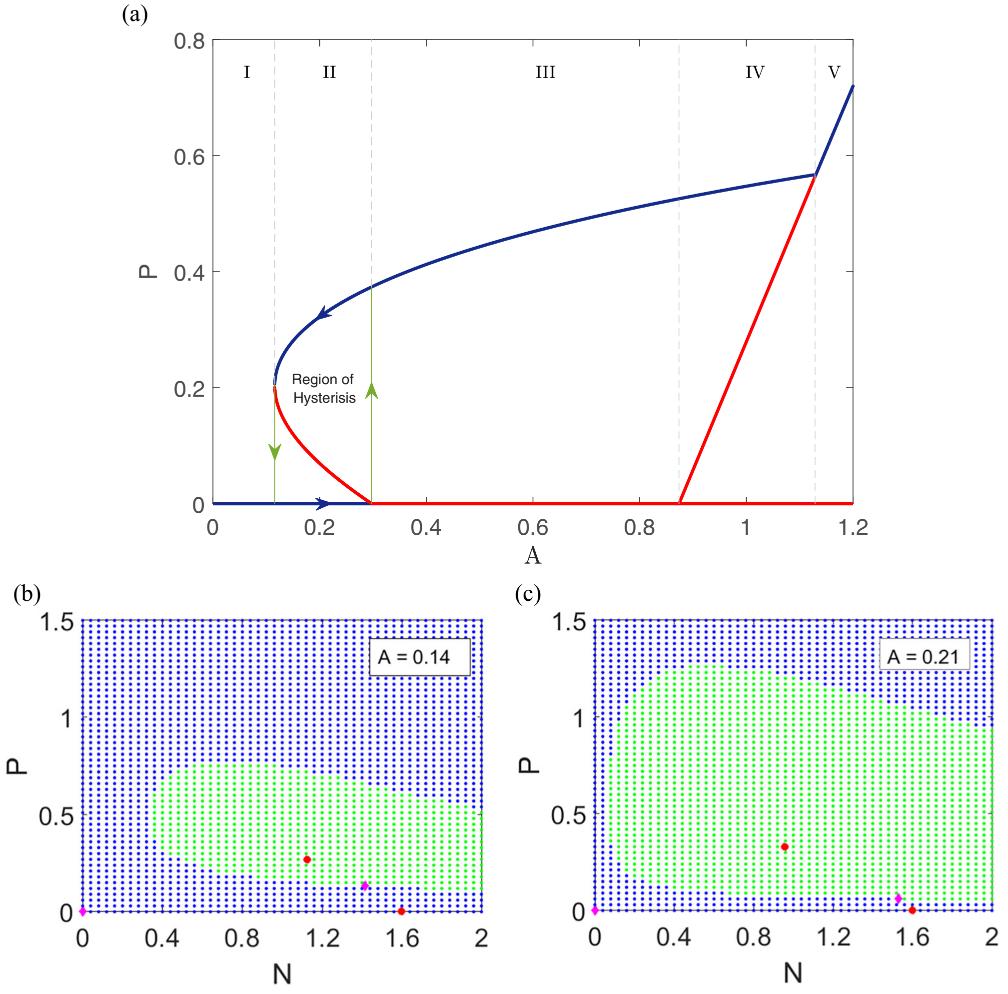

FIG. 4. (a) Backward bifurcation of the system (1) with respect to additional food quantity A with $m = 0.68$ and $\alpha = 1.05$. The hysteresis loop is represented by arrows. Also shown are the basins of attraction of the equilibria (b) $E_1^*(1.1248, 0.2686)$ (green) and $E_1(1.6, 0)$ (blue) for $A = 0.14$ and (c) $E_1^*(0.9571, 0.3286)$ (green) and $E_1(1.6, 0)$ (blue) for $A = 0.21$.

of attraction of the coexistence equilibrium. Therefore, an increase in the additional food quantity A reduces the possibility of predator extinction from the ecosystem.

2. *Elevated strength of cooperative hunting induces different types of bistabilities*

Figure 5(a) shows that for $\alpha < 0.7189$ the system (1) possesses no biologically feasible interior equilibrium. A pair of coexisting equilibria E_1^* and E_2^* emerge through a saddle-node bifurcation when α crosses the threshold $\alpha = 0.7189$. However, strong predation pressure on prey due to elevated cooperative intensity decreases prey density, which in turn becomes detrimental to predators. The equilibrium position E_2^* is always unstable, whereas E_1^* exchanges its stability and produces a periodic phenomenon via a Hopf bifurcation at $\alpha = 2.374$. In the parameter window $\alpha \in (0.7189, 2.374)$, the system experiences bistability between the coexisting steady state with higher predator biomass and a predator-free state. The population cycles develop rapidly until it experiences a collision with the coexisting steady state with lower predator density. Then the oscillations are suddenly wiped out via a homoclinic bifurcation at $\alpha = 6.829$. Therefore, the system exhibits another type of bistability between periodic cycles and the predator-free equilibrium for $\alpha \in (2.374, 6.829)$. Thus, strong cooperation intensities hamper the stable coexistence of interacting populations. Strong hunting cooperation decreases the domain of the basin of attraction of the coexistence equilibrium (figure is not shown). The hump-shaped equilibrium curve supports that the beneficial impact of strong cooperative hunting on predator population is overcompensated by the decline in prey density.

3. *Prey refuge size promotes sudden collapse of coexistence scenario*

Now we explore the bifurcation scenario and stability patterns of the system when multiple coexisting equilibrium states exist, considering variations in the prey refuge size m [Fig. 5(b)]. The predator-free equilibrium E_1 is unstable for $m < m^* = 0.5979$ and stable if $m > m^*$. For $m < m^*$, there is a unique coexisting steady state, which is a local attractor. At $m = m^*$, another coexisting state originates in the forward route from E_1. For $m^* < m < \bar{m}$, where $\bar{m}$ is approximately 0.6961, there are two coexistence equilibria, but at $m = \bar{m}$,

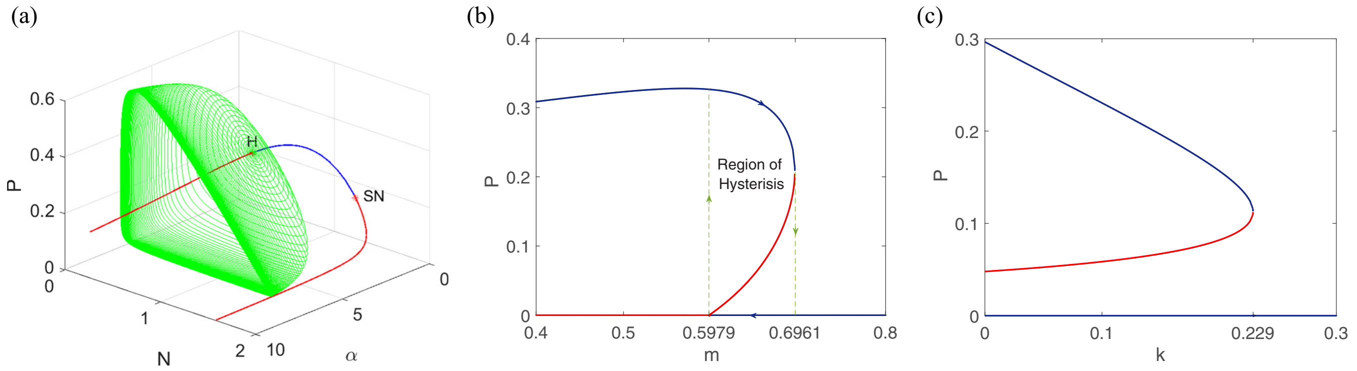

FIG. 5. (a) Saddle-node and homoclinic bifurcations of the system (1) with respect to α for $m = 0.65$ and $A = 0.15$. (b) Backward and saddle-node bifurcations with respect to m for $A = 0.15$ and $\alpha = 1.05$. (c) The predator experiences catastrophic extinction with respect to k ($=k_1 = k_2$) for $\alpha = 0.65$, $m = 0.62$, and $A = 0.15$. The hysteresis loop is depicted by arrows.

they coalesce and disappear, and for $m > \bar{m}$, no coexistence is captured.

4. *Increased fear of predation risk increases the likelihood of predator extinction*

Next we discuss a situation in which the ecological system exhibits a pair of coexisting steady states in the absence of the fear factor [Fig. 5(c)]. Numerical computations explore that for $k \in [0, 0.229]$, one interior equilibrium E_1^* is stable and another E_2^* is unstable. In this parameter window, the solution settles to either a predator-free state or the coexistence of both populations depending upon initial densities. Notably, above the threshold level $k = 0.229$, these two equilibria annihilate. Therefore, a gradual increment in the fear level k may induce sudden predator extinction in the system.

V. STOCHASTIC MODEL

Several stochastic population dynamic frameworks adopt the assumption of temporally uncorrelated noise for mathematical simplicity. However, it is noteworthy that in real ecological systems, environmental fluctuations tend to exhibit positive autocorrelation [38]. This motivates us to model environmental stochasticity as an autocorrelated process. We propose the stochastic model as

$$\frac{dX}{dt} = \psi(X) + X\xi(t), \tag{5}$$

where $X = [N, P]^T$ and $\psi(X)$ is the corresponding deterministic skeleton. The value of a colored noise random field at any given location may be independent, but it exhibits correlations with the values of that field at other locations. Here we address the Gaussian stochastic process ξ that exhibits a temporal autocorrelation characterized by a $1/f^\beta$ frequency spectrum. The $1/f^\beta$ model characterizes perturbations with a memory component. Under the framework of $1/f^\beta$ noise, the correlation in the ξ values at two distinct time points is diminished following a power-law pattern, signifying that the correlation is proportional to a power of the time interval. As the redness of noise β increases, the noise realizations exhibit greater "smoothness," indicating an escalating correlation within the random field.

We term this formulation multiplicative noise because $\xi(t)$ is multiplied by a population density-dependent function (in this case, X). While alternative approaches, such as additive noise [39], can be employed to represent stochasticity, the more prevalent practice in ecological modeling is to incorporate environmental fluctuations by multiplying the noise term by the state variable [40,41]. In this scenario, fluctuations around low-density states are notably diminished, and when the state reaches zero, the noise component will disappear. Multiplicative noise accounts for perturbations that have a per capita impact, such as random variations in survivorship or fecundity.

A. Stochastic simulation

We perform stochastic simulations in MATLAB employing the Euler-Maruyama method [42]. A time span of 20 000 units is taken into account to encompass the overall configuration of the stochastic counterpart. The step size of integration is set as $\Delta t = 1$. We increase the redness of noise to explore how the system dynamics alters with lag-1 autocorrelation elevation. We produce a stochastic signal with spectral exponent β utilizing the algorithm outlined in [43]. Here $\beta \to 0$ indicates white noise while $\beta > 0$ captures redshifted (positively autocorrelated) noise.

1. *Time-series analysis*

In the absence of noise or with white or pale red noise ($\beta \approx 0$) with low intensity, the system tends to visit the coexisting attractor depending upon initial conditions and remains in its vicinity (see Fig. 6). In the case of white noise, an elevation in noise intensity drives the population densities to fluctuate in a wider range around the deterministic steady state (0.8253,0.3849). With moderate noise intensity, as we increase the redness of noise, the time series shows an attractor-switching behavior between the coexisting and predator-free states. Interestingly, the residence time at the predator-free attractor is relatively short, and the populations predominantly remain around their respective equilibrium densities at the coexisting steady state for the majority of time. High-intensity redshifted noise induces a similar dynamical scenario. However, in this case, the residence time at the boundary attractor increases and the system spends significant

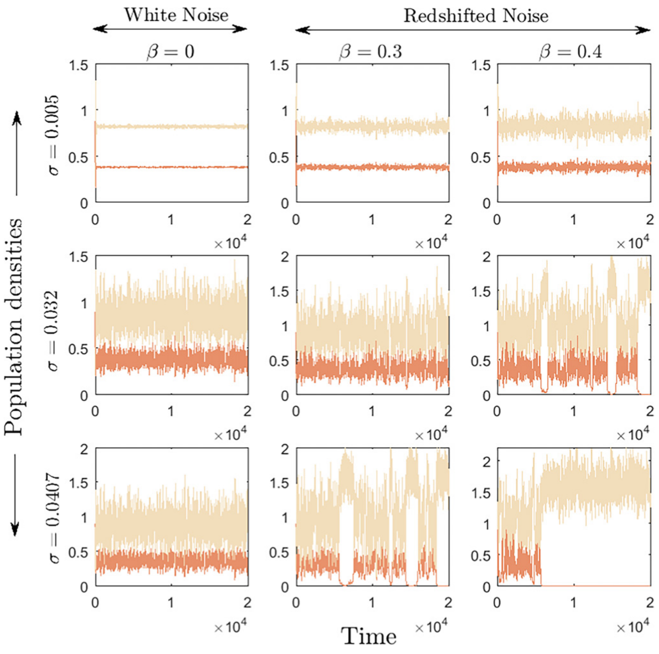

FIG. 6. Time evolutions of the stochastic system (5) for different noise intensities σ and colors β. The parameters are taken from Table I except for $\beta_1 = 1.1$, $m = 0.68$, $A = 0.3528$, and $\alpha = 1.05$. Yellow and orange represent the prey and predator densities, respectively.

time near the attractor (1.6,0). For high-enough intensity σ with increased redness, the time evolutions initially fluctuating around the deterministic coexisting state jump to the predator-extinction state and reside there.

2. *Transitions from changes in control parameters*

To investigate the transitions resulting from variations in additional food quantity and quality, we have conducted simulations by uniformly changing the control parameters β_1 and A over a span of 20 000 time units. To facilitate comparison, we have included the deterministic bifurcation diagrams in the same figure. The number of possible feasible interior equilibria is one, two, or zero according to $0 < \beta_1 < 1$, $1 < \beta_1 < 4.0702$, or $\beta_1 > 4.0702$, respectively. The system undergoes a backward bifurcation at $\beta_1 = 1$. The predator equilibrium density decreases with increasing β_1. Interestingly, predators experience catastrophic eradication around a saddle-node bifurcation at $\beta_1 = 4.0702$ and the prey population reaches its carrying capacity.

Under environmental stochasticity, we observe critical transitions by decreasing additional food quality over time for a fixed intensity of white noise [Fig. 7(a)]. However, an increase in intensity or redness of noise results in such a transition far before the tipping point [Figs. 7(b) and 7(c)]. We document a noncatastrophic pattern of prey eradication with an increase in additional food quantity [Figs. 7(d)–7(f)].

3. *Confidence ellipse analysis: White noise case*

In recent decades, extensive research has been conducted on deterministic models featuring transitions induced by noise [44,45]. Bashkirtseva *et al.* [46] introduced a novel approach that utilizes the stochastic sensitivity function (SSF) technique for constructing analytical descriptions of randomly forced equilibria and cycles in discrete-time models. Multistable systems demonstrate intricate dynamics characterized by noise-induced hopping between attractors and their respective basins of attraction [47]. Analyzing the sensitivity of randomly forced oscillations is crucial for the investigation of these transitions. Utilizing the SSF technique [48], we construct confidence ellipses to characterize the phenomenon of noise-induced state switching between two stochastic equilibria. Subsequently, we estimate the tipping threshold σ_T.

Define

$$F = \begin{pmatrix} f_{11} & f_{12} \\ f_{21} & f_{22} \end{pmatrix}, \quad G = \begin{pmatrix} g_{11} & 0 \\ 0 & g_{22} \end{pmatrix}, \quad S = GG^T,$$

where

$$f_{ij} = c_{ij}, \quad g_{11} = N^*, \quad g_{22} = P^*.$$

Let W be the stochastic sensitivity matrix

$$W = \begin{pmatrix} w_{11} & w_{12} \\ w_{21} & w_{22} \end{pmatrix},$$

which satisfies the equations

$$\begin{aligned} 2f_{11}w_{11} + f_{12}w_{12} + f_{12}w_{21} &= -g_{11}^2, \\ f_{21}w_{11} + (f_{11} + f_{22})w_{12} + f_{12}w_{22} &= 0, \\ f_{21}w_{11} + (f_{11} + f_{22})w_{21} + f_{12}w_{22} &= 0, \\ f_{21}w_{12} + f_{21}w_{21} + 2f_{22}w_{22} &= -g_{22}^2. \end{aligned}$$

Employing (A.3) in [49], the equation of confidence ellipse is given by

$$\begin{aligned} &\langle (x - N^*, y - P^*)^T, W^{-1}(x - N^*, y - P^*)^T \rangle \\ &= 2\sigma^2 \ln\left(\frac{1}{1-p}\right), \end{aligned} \tag{6}$$

where p represents the fiducial probability. At the attractor $E_1^* = (0.9708, 0.3548)$, the stochastic sensitivity matrix and its inverse are obtained as

$$W = \begin{pmatrix} 22.4813 & -6.3349 \\ -6.3349 & 4.0697 \end{pmatrix},$$

$$W^{-1} = \begin{pmatrix} 0.0792 & 0.1233 \\ 0.1233 & 0.4377 \end{pmatrix}.$$

From (6), the equation of confidence ellipse at E_1^* is given by

$$\begin{aligned} &0.0792(x - 0.9708)^2 + 0.2466(x - 0.9708)(y - 0.3548) \\ &+ 0.4377(y - 0.3548)^2 = 2\sigma^2 \ln\left(\frac{1}{1-p}\right). \end{aligned} \tag{7}$$

Fixing the fiducial probability at $p = 0.95$, we calibrate different noise intensities $\sigma = 0.025$, 0.059, and 0.067. The corresponding confidence ellipses are depicted in Fig. 8(a). It is noteworthy that as the noise intensity increases, the confidence ellipse expands and enters the attraction domain of the predator-free equilibrium after crossing the separatrix. The value of σ at which the confidence ellipse tangentially meets the separatrix serves as an estimate for the threshold noise marking the onset of noise-induced transitions. In our case, the

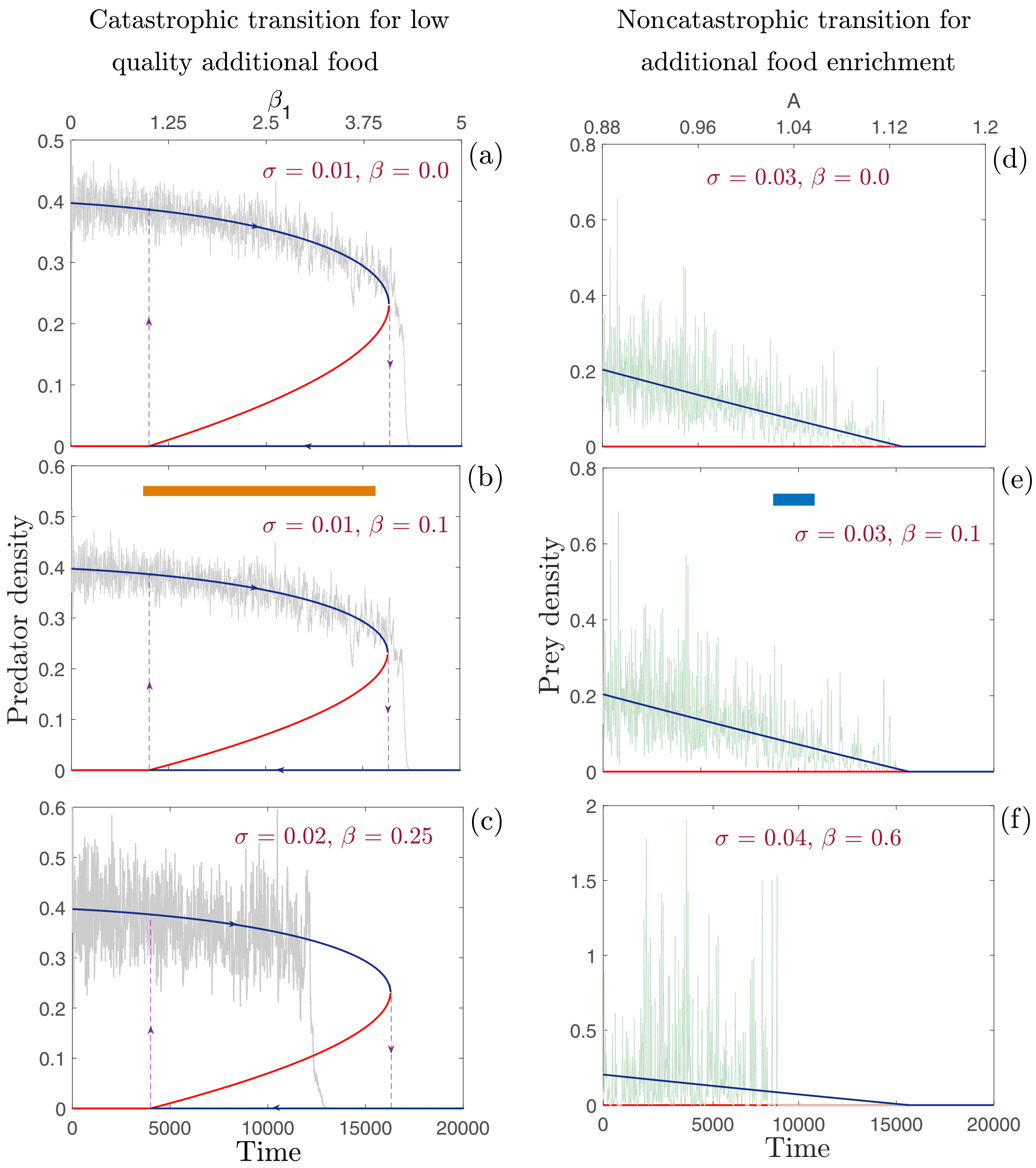

FIG. 7. (a)–(c) Bifurcation-induced tipping driven by variation in additional food quality β_1. (d)–(f) Critical transitions for varying additional food quantity A. The control parameters are varied over the time window $t \in [0, 20\,000]$ for different combinations of σ and β. Parameter values are the same as in Fig. 6.

tipping threshold is estimated as $\sigma = \sigma_T = 0.059$. Figure 8(b) showcases the confidence ellipse with $\sigma = 0.03$, demonstrating that the stochastic model's random states are distributed around the associated deterministic coexistence equilibrium. Furthermore, these states lie within the confidence ellipse with probability 0.95.

4. Early warning signals

We have observed that when the quality of additional food A deteriorates, i.e., if the predator takes longer to handle additional food compared to the basal resource, the predator population undergoes an abrupt collapse within the ecosystem via a saddle-node bifurcation. Furthermore, with an increase in additional food quantity β_1 for predators, the prey density drops and eventually vanishes. This noncatastrophic collapse of prey population is characterized by the emergence of a transcritical bifurcation. The propensity of the proposed ecological model to exhibit early warning signals (EWSs) before a shift varies significantly when transitions are driven by alterations in the control parameters β_1 and A. To achieve stationary residuals, we apply Gaussian detrending with bandwidth 5 to the time series prior to analysis. We compute the variance and lag-1 autocorrelation with window size equal to 60% of the pretransition data. For both types of transitions, we estimate the rise of EWSs utilizing Kendall's τ. Prior to the saddle-node bifurcation, both variance and autocorre-

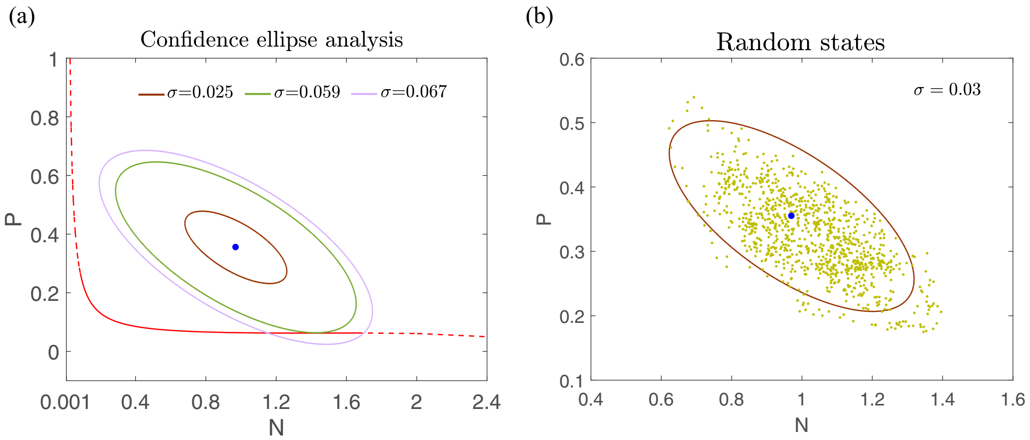

FIG. 8. (a) Separatrix (red dashed curve) of the basins of attraction of the equilibria $E_1^*(0.971, 0.3548)$ and $E_1(1.6, 0)$ and confidence ellipses for different intensities σ of white noise ($\beta_1 = 0$). (b) Random states (green dots) and confidence ellipse (brown curve) for $\sigma = 0.03$ and $\beta_1 = 0$. The rest of the parameters are at the same levels as in Fig. 7(a) with $\beta_1 = 2.5$.

lation consistently experience an upward trend (see Fig. 9). However, in the case of the transcritical bifurcation, these indicators do not follow the same pattern.

VI. RESULTS AND DISCUSSION

In our present investigation, we have taken into account the impact of hunting cooperation among predators, which induces a heightened fear of predation in the prey species. Predator incited fear compels the prey to migrate temporarily to a substandard-quality zone. Due to insufficient resources, predators switch to additional food supplements to withstand their extinction. In our mathematical analysis, we first examined the feasibility of possible equilibria in the ecological system. Subsequently, we established the sufficient conditions that guarantee the local stability of these steady states.

We investigated how different strengths of cooperative hunting affect predator density, predator survival, and the stability scenario of the ecological configuration. We observed that when predators cooperate weakly, the captured prey biomass is not sufficient for their survival. When the predator cooperation strength increases, it is possible that predator interference surpasses foraging facilitation, leading to a hump-shaped relationship between the degree of cooperation and predator biomass. Ecologically, the hump-shaped curve illustrates that a certain level of cooperation can enhance foraging efficiency and consequently lead to a higher predator population. However, increased predation pressure on prey due to elevated cooperation intensity decreases prey density, which becomes detrimental to predators. Recently, Biswas and Mandal [9] studied a prey-predator model with infection and revealed that the cooperation intensity can by itself induce the phenomenon of bistability between the disease-free and disease-dominated states. Here we observed the oscillatory coexistence of interacting populations in intermediate ranges of cooperation intensity. The elevated intensity may prevent the abruptly increasing oscillations through the onset of a homoclinic bifurcation. As a result, the system transitions to a state of monostability and converges towards the predator-free environment. Different types of bistability scenarios reflect sensitivity of the proposed model to small perturbations. Interestingly, we found that the beneficial effect of a strong prey refuge is overcompensated by the decrease in predator density. Previous empirical literature documented that predator population decreases continuously as a consequence of prey refuge and eventually experiences complete eradication through a transcritical bifurcation [21,29,50]. However, we observed that with a high amount of prey refuge, due to a shortage of basal resources, the predator population experiences an extreme risk of catastrophic collapse. Sk *et al.* [51] investigated a predator-prey system with additional food and concluded that ample availability of additional food helps control population fluctuations. In contrast, we obtained more complicated dynamical scenarios in terms of both additional food quantity and quality. We observed the onset of twofold coexisting equilibria through a saddle-node bifurcation with varying quantity of additional food. This type of bifurcation leads to a potential regime shift, whereby a minute alteration in additional food quantity may result in an abrupt state transition from a predator-free to a predator-dominated configuration or vice versa. Notably, a huge amount of additional food for predators is not conducive to the survival of basal prey. The quality of additional food also determines the fate of predators. As the quality of additional food continues to decrease, the predator experiences a sudden collapse from the ecosystem. However, the fear phenomenon affecting the prey's reproductive success and mortality causes a significant decline in prey biomass. Scarcity of the focal resource drives the predator density to a low level. This outcome agrees with that in [50]. If the additional food is available at a high concentration, due to predator abundance, the impact of nonconsumptive risk becomes more effective. Under these circumstances, the prey density drops rapidly and eventually undergoes a sudden collapse.

We observed that the population densities exhibit a wider range of fluctuations around the deterministic steady state due to the influence of noise intensity σ. In the case of moderate noise intensity, augmenting the redness of the noise β reveals the occurrence of noise-induced stochastic switching dynamics between the coexisting and predator-free states within the region of bistability. As the intensity of the noise

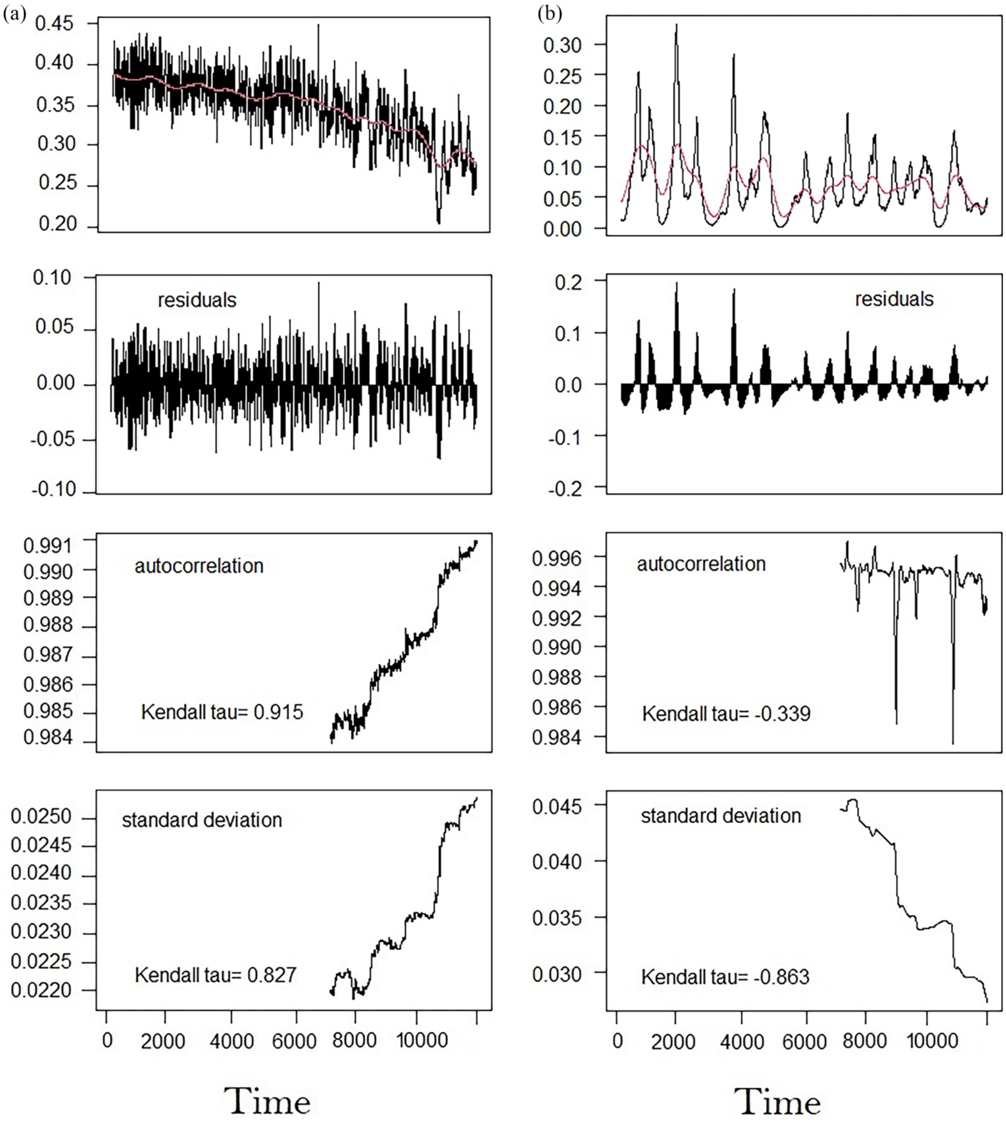

FIG. 9. Early warning signals for transitions of the stochastic model (5) with redshifted noise driven by changes in (a) additional food quality β_1 and (b) quantity A. The results are obtained using (a) $t = 3700–15\,700$ from Fig. 7(b) (red segment) and (b) $t = 8700–10\,700$ from Fig. 7(e) (blue segment). We calculated variance and autocorrelation within rolling windows of 60% the size of the time-series segments.

increases further with increased redness, the time evolutions initially characterized by fluctuations around the deterministic coexisting state eventually transition towards the predator-extinction state. We have employed a confidence ellipse analysis technique to estimate the tipping threshold σ_T of the white noise intensity. In a noisy environment, we observed critical transitions by decreasing (increasing) additional food quality (quantity) over time. However, an escalation in noise intensity or redness triggers these transitions to occur well before reaching the tipping point. In summary, generic early warning indicators can successfully predict the imminent catastrophic extinction of predators resulting from a low-quality diet. However, these indicators fail to forecast the noncatastrophic transitions that lead to the extinction of prey species in the presence of abundant additional food for predators. Therefore, in environments enriched with additional food sources, conservation management efforts may encounter challenges in effectively preserving both the predators and their basal resources simultaneously.

In the context of prey-predator systems, supplying additional food to stabilize prey populations draws parallels with interventions like vaccinations and monetary policies, aimed to stabilize and prevent crises. External interventions encompass feedback loops that amplify or dampen their impacts, resulting in dynamic behaviors, such as economic growth or reduced disease transmission. However, introducing additional resources or interventions can yield unexpected repercussions, akin to overpopulation of predators or alterations in prey behavior. In both prey-predator and human systems, resilience and adaptation are observed when additional resources are introduced, potentially leading to new steady states or behaviors. For example, social safety nets help individuals adapt to economic shocks. Understanding these analogies can inform decision-making in various fields and help mitigate unintended consequences when making interventions in complex systems.

Providing additional resources without ensuring their quality or proper management can lead to adverse outcomes, analogous to the predator becoming extinct in a low-quality additional food scenario. For example, use of excessive and substandard-quality resources (antibiotics) to combat infections can possess negative consequences, impacting the overall healthcare system. If low-quality subsidies are offered without any proper strategy, it might not stimulate economic growth as expected. This can lead to economic instability and long-term negative effects on the economic system. This emphasizes the importance of thoughtful planning, quality assurance, and strategic resource allocation in various domains to achieve positive and sustainable outcomes.

ACKNOWLEDGMENTS

The authors would like to thank Sagar Karmakar (Agricultural and Ecological Research Unit, Indian Statistical Institute, India) for thoughtful discussions and productive conversations.

[1] K. J. Flynn, How critical is the critical N:P ratio? J. Phycol. **38**, 961 (2002).

[2] S. G. Leles, J. L. Valentin, and G. M. Figueiredo, Evaluation of the complexity and performance of marine planktonic trophic models, An. Acad. Bras. Cienc. **88**, 1971 (2016).

[3] S. Creel and N. M. Creel, Communal hunting and pack size in African wild dogs, *Lycaon pictus*, Anim. Behav. **50**, 1325 (1995).

[4] K. B. Altendorf, J. W. Laundré, C. A. López González, and J. S. Brown, Assessing effects of predation risk on foraging behavior of mule deer, J. Mammal. **82**, 430 (2001).

[5] W. J. Ripple and R. L. Beschta, Wolves and the ecology of fear: Can predation risk structure ecosystems? BioScience **54**, 755 (2004).

[6] F. Hua, K. E. Sieving, R. J. Fletcher, Jr., and C. A. Wright, Increased perception of predation risk to adults and offspring alters avian reproductive strategy and performance, Behav. Ecol. **25**, 509 (2014).

[7] X. Wang, L. Zanette, and X. Zou, Modelling the fear effect in predator-prey interactions, J. Math. Biol. **73**, 1179 (2016).

[8] S. Biswas, P. K. Tiwari, and S. Pal, Delay-induced chaos and its possible control in a seasonally forced eco-epidemiological model with fear effect and predator switching, Nonlinear Dyn. **104**, 2901 (2021).

[9] S. Biswas and A. Mandal, Cooperation-mediated regime shifts in a disease-dominated prey–predator system, Chaos Soliton. Fract. **170**, 113352 (2023).

[10] J. Duarte, C. Januário, N. Martins, and J. Sardanyés, Chaos and crises in a model for cooperative hunting: A symbolic dynamics approach, Chaos **19**, 043102 (2009).

[11] M. T. Alves and F. M. Hilker, Hunting cooperation and Allee effects in predators, J. Theor. Biol. **419**, 13 (2017).

[12] S. Pal, N. Pal, S. Samanta, and J. Chattopadhyay, Effect of hunting cooperation and fear in a predator-prey model, Ecol. Complexity **39**, 100770 (2019).

[13] J. Liu, B. Liu, P. Lv, and T. Zhang, An eco-epidemiological model with fear effect and hunting cooperation, Chaos Soliton. Fract. **142**, 110494 (2021).

[14] E. González-Olivares and R. Ramos-Jiliberto, Dynamic consequences of prey refuges in a simple model system: more prey, fewer predators and enhanced stability, Ecol. Model. **166**, 135 (2003).

[15] G. Sagrario, M. D. LosÁngeles, E. Balseiro, R. Ituarte, and E. Spivak, Macrophytes as refuge or risky area for zooplankton: A balance set by littoral predacious macroinvertebrates, Freshwater Biol. **54**, 1042 (2009).

[16] S. Biswas, P. K. Tiwari, F. Bona, S. Pal, and E. Venturino, Modeling the avoidance behavior of zooplankton on phytoplankton infected by free viruses, J. Biol. Phys. **46**, 1 (2020).

[17] S. Biswas, P. K. Tiwari, Y. Kang, and S. Pal, Effects of zooplankton selectivity on phytoplankton in an ecosystem affected by free-viruses and environmental toxins, Math. Biosci. Eng. **17**, 1272 (2020).

[18] S. Biswas, P. K. Tiwari, and S. Pal, Effects of toxicity and zooplankton selectivity on plankton dynamics under seasonal patterns of viruses with time delay, Math. Methods Appl. Sci. **45**, 585 (2022).

[19] S. Sharma and G. P. Samanta, A Leslie–Gower predator–prey model with disease in prey incorporating a prey refuge, Chaos Soliton. Fract. **70**, 69 (2015).

[20] J. N. McNair, The effects of refuges on predator-prey interactions: A reconsideration, Theor. Popul. Biol. **29**, 38 (1986).

[21] T. K. Kar, Stability analysis of a prey-predator model incorporating a prey refuge, Commun. Nonlinear Sci. Numer. Simul. **10**, 681 (2005).

[22] P. D. N. Srinivasu and B. S. R. V. Prasad, Role of quantity of additional food to predators as a control in predator-prey systems with relevance to pest management and biological conservation, Bull. Math. Biol. **73**, 2249 (2011).

[23] G. R. Huxel and K. McCann, Food web stability: The influence of trophic flows across habitats, Am. Nat. **152**, 460 (1998).

[24] B. Vandekerkhove and P. De Clercq, Pollen as an alternative or supplementary food for the mirid predator *Macrolophus pygmaeus*, Biol. Control **53**, 238 (2010).

[25] K. D. Lafferty and A. M. Kuris, Biological control of marine pests, Ecology **77**, 1989 (1996).

[26] M. R. Wade, M. P. Zalucki, S. D. Wratten, and K. A. Robinson, Conservation biological control of arthropods using artificial food sprays: Current status and future challenges, Biol. Control **45**, 185 (2008).

[27] L. Gibson, The role of lethal control in managing the effects of apparent competition on endangered prey species, Wildl. Soc. Bull. **34**, 1220 (2006).

[28] P. D. N. Srinivasu, B. S. R. V. Prasad, and M. Venkatesulu, Biological control through provision of additional food to predators: A theoretical study, Theor. Popul. Biol. **72**, 111 (2007).

[29] A. Mandal, P. K. Tiwari, and S. Pal, A nonautonomous model for the effects of refuge and additional food on the dynamics of phytoplankton-zooplankton system, Ecol. Complexity **46**, 100927 (2021).

[30] B. Sahoo and S. Poria, The chaos and control of a food chain model supplying additional food to top-predator, Chaos Soliton. Fract. **58**, 52 (2014).

[31] A. Mandal, P. K. Tiwari, S. Samanta, E. Venturino, and S. Pal, A nonautonomous model for the effect of environmental toxins on plankton dynamics, Nonlinear Dyn. **99**, 3373 (2020).

[32] P. J. Rasch, S. Tilmes, R. P. Turco, A. Robock, L. Oman, C. C. Chen, G. L. Stenchikov, and R. R. Garcia, An overview of geoengineering of climate using stratospheric sulphate aerosols, Philos. Trans. R. Soc. A **366**, 4007 (2008).

[33] C. T. Bauch and S. Bhattacharyya, Evolutionary game theory and social learning can determine how vaccine scares unfold, PLoS Comput. Biol. **8**, e1002452 (2012).

[34] Y. Sawada and Y. Takasaki, Natural disaster, poverty, and development: An introduction, World Dev. **94**, 2 (2017).

[35] V. Guttal and C. Vishwesha, Impact of noise on bistable ecological systems, Ecol. Model. **201**, 420 (2007).

[36] S. Sarkar, A. Narang, S. K. Sinha, and P. S. Dutta, Effects of stochasticity and social norms on complex dynamics of fisheries, Phys. Rev. E **103**, 022401 (2021).

[37] D. Mukherjee, Role of fear in predator-prey system with intraspecific competition, Math. Comput. Simul. **177**, 263 (2020).

[38] J. M. Halley, Ecology, evolution and $1/f$-noise, Trends Ecol. Evol. **11**, 33 (1996).

[39] S. Kéfi, V. Dakos, M. Scheffer, E. H. Van Nes, and M. Rietkerk, Early warning signals also precede non-catastrophic transitions, Oikos **122**, 641 (2013).

[40] S. N. Evans, P. L. Ralph, S. J. Schreiber, and A. Sen, Stochastic population growth in spatially heterogeneous environments, J. Math. Biol. **66**, 423 (2013).

[41] Y. Sharma, K. C. Abbott, P. S. Dutta, and A. K. Gupta, Stochasticity and bistability in insect outbreak dynamics, Theor. Ecol. **8**, 163 (2015).

[42] D. J. Higham, An algorithmic introduction to numerical simulation of stochastic differential equations, SIAM Rev. **43**, 525 (2001).

[43] M. Stoyanov, M. Gunzburger, and J. Burkardt, Pink noise, $1/f^{\alpha}$ noise, and their effect on solutions of differential equations, Int. J. Uncertainty Quantif. **1**, 257 (2011).

[44] C. Xu, S. Yuan, and T. Zhang, Stochastic sensitivity analysis for a competitive turbidostat model with inhibitory nutrients, Int. J. Bifurcat. Chaos **26**, 1650173 (2016).

[45] D. Wu, H. Wang, and S. Yuan, Stochastic sensitivity analysis of noise-induced transitions in a predator-prey model with environmental toxins, Math. Biosci. Eng. **16**, 2141 (2019).

[46] I. Bashkirtseva, L. Ryashko, and I. Tsvetkov, Sensitivity analysis of stochastic equilibria and cycles for the discrete dynamic systems, Dyn. Contin. Discrete Impuls. Syst. A **17**, 501 (2010).

[47] S. Kraut and U. Feudel, Multistability, noise, and attractor hopping: The crucial role of chaotic saddles, Phys. Rev. E **66**, 015207(R) (2002).

[48] J. Gao, J. Ji, Y. Liu, F. Zhang, R. Wang, and H. Wang, A confidence ellipse analysis for stochastic dynamics model of Alzheimer's disease, Nonlinear Dyn. **111**, 13513 (2023).

[49] I. Bashkirtseva, T. Ryazanova, and L. Ryashko, Confidence domains in the analysis of noise-induced transition to chaos for Goodwin model of business cycles, Int. J. Bifurc. Chaos **24**, 1440020 (2014).

[50] H. Zhang, Y. Cai, S. Fu, and W. Wang, Impact of the fear effect in a prey-predator model incorporating a prey refuge, Appl. Math. Comput. **356**, 328 (2019).

[51] N. Sk, P. K. Tiwari, S. Pal, and M. Martcheva, A delay non-autonomous model for the combined effects of fear, prey refuge and additional food for predator, J. Biol. Dyn. **15**, 580 (2021).